JPSE (Journal of Physical Science and Engineering), Vol. 9, No. 2, 2024, Page 114–120.
DOI: 10.17977/um024v9i22024p114-120

JPSE
(Journal of Physical Science and Engineering)

http://journal2.um.ac.id/index.php/jpse
EISSN: 2541-2485

Flow-Rate-Regulated Co-Precipitation via Peristaltic Pump for Controlled Nucleation and Morphology of ZnO Nanorods

Received
28 August 2024

Revised
12 October 2024

Accepted for Publication
16 October 2024

Published
31 October 2024

Thathit Suprayogi[1]*, Samsul Arifin[1], Sudarman Rahman[2], Mu'afa Purwa Arsana[3], Rokiy Alfanaar[4], Awalul Fatiqin[5], Yahya Febrianto[2]

1. Department of Physics, Faculty of Mathematics and Natural Sciences, Universitas Palangka Raya, Palang Raya 73111, Central Kalimantan, Indonesia
2. Department of Pharmacy, Faculty of Mathematics and Natural Sciences, Universitas Palangka Raya, Palang Raya 73111, Central Kalimantan, Indonesia
3. Department of Mathematics, Faculty of Mathematics and Natural Sciences, Universitas Palangka Raya, Palang Raya 73111, Central Kalimantan, Indonesia
4. Department of Chemistry, Faculty of Mathematics and Natural Sciences, Universitas Palangka Raya, Palang Raya 73111, Central Kalimantan, Indonesia
5. Department of Biology, Faculty of Mathematics and Natural Sciences, Universitas Palangka Raya, Palang Raya 73111, Central Kalimantan, Indonesia

***E-mail:** thathit.suprayogi@mipa.upr.ac.id

Abstract
This study presents a flow-rate-regulated co-precipitation method for synthesizing ZnO nanoparticles using a peristaltic pump to enhance control over nucleation and growth processes. The primary objective was to investigate the effect of controlled reactant delivery on the structural and morphological properties of ZnO nanoparticles. A peristaltic pump system was calibrated to provide a stable and continuous flow of the precipitating agent, achieving an average flow rate of 93.39 ± 1.39 µL/s with high linearity ($R^2 = 0.99946$). ZnO nanoparticles were synthesized under controlled conditions and characterized using X-ray diffraction (XRD) and scanning electron microscopy (SEM). The XRD results confirmed the formation of a single-phase hexagonal ZnO structure with high crystallinity and an average crystallite size of 55.98 ± 8.35 nm. SEM analysis revealed the formation of nanorod structures with relatively uniform morphology. The improved uniformity is attributed to stable supersaturation conditions enabled by precise flow-rate control. These findings demonstrate that flow-rate regulation is a critical parameter in co-precipitation synthesis and offers a simple, cost-effective strategy for improving reproducibility and structural control in nanoparticle fabrication.

Keywords: ZnO nanoparticles, co-precipitation, peristaltic pump, flow-rate control, nanorods.

1. Introduction

Zinc oxide (ZnO) nanoparticles have emerged as one of the most extensively investigated semiconductor nanomaterials due to their unique physicochemical properties, including a wide direct band gap (~3.37 eV), high exciton binding energy (~60 meV), and strong photocatalytic and antimicrobial activity. These characteristics make ZnO highly suitable for applications in optoelectronics, gas sensors, photocatalysis, energy conversion, and biomedical systems [1]–[4]. The versatility of ZnO nanostructures has driven significant research efforts aimed at tailoring their structural and functional properties for specific technological applications.

The performance of ZnO nanoparticles in such applications is strongly dependent on their crystallinity, particle size, morphology, and surface characteristics. For example, nanorod and nanosheet morphologies exhibit enhanced surface area and anisotropic charge transport properties, which are advantageous for photocatalytic and sensing applications [5]–[7]. Consequently, precise control over nanoparticle synthesis is essential to optimize these functional properties and achieve reproducible performance.

Various synthesis techniques have been developed to produce ZnO nanoparticles, including sol–gel, hydrothermal, chemical vapor deposition, and co-precipitation methods. Among these, co-precipitation is particularly attractive due to its simplicity, low cost, scalability, and relatively mild reaction conditions [8]–[10]. These advantages make it suitable for large-scale production and practical industrial applications. Despite its advantages, the co-precipitation method suffers from a fundamental limitation: poor control over nucleation and growth kinetics. In conventional processes, the precipitating agent is typically added manually via dropwise addition using a burette or pipette. This approach introduces fluctuations in local supersaturation, leading to uncontrolled nucleation, particle aggregation, and broad size distribution. As a result, achieving consistent and reproducible nanoparticle properties remains challenging.

Recent studies have highlighted that mixing dynamics and reactant delivery rate play a crucial role in determining supersaturation levels and nucleation behavior [11], [12]. However, systematic investigations focusing on precise flow-rate-controlled co-precipitation systems are still limited. In particular, the relationship between controlled reactant flow and nanoparticle morphology, crystallinity, and size distribution has not been thoroughly explored [13]. To overcome these limitations, this study proposes the integration of a peristaltic pump into the co-precipitation process to enable continuous and controlled addition of the precipitating agent [14]. Unlike conventional manual methods, a peristaltic pump provides stable, programmable, and reproducible flow rates, thereby minimizing fluctuations in local supersaturation. This approach is expected to significantly improve control over nucleation kinetics and particle growth mechanisms.

This work provides a novel yet cost-effective strategy for enhancing reproducibility in wet-chemical nanoparticle synthesis. By establishing the role of flow-rate control as a key parameter in governing nanoparticle formation, this study contributes to a deeper mechanistic understanding of co-precipitation processes. Furthermore, the proposed approach has the potential to be extended to other metal oxide systems, offering a scalable pathway toward high-quality nanomaterial production for advanced technological applications.

2. Method

5.1. Materials

Zinc acetate dihydrate ($Zn(CH_3COO)_2{\cdot}2H_2O$, ≥99% purity) was used as the zinc precursor, while sodium hydroxide (NaOH, ≥98%) served as the precipitating agent. All reagents were of analytical grade and used without further purification. Distilled water was used as the solvent throughout the experiments.

5.2. Experimental Setup and System Configuration

The synthesis system consisted of a magnetic stirrer with a hotplate, a peristaltic pump, a DC voltage controller, a regulated power supply, and a reaction vessel (250 mL glass beaker). The peristaltic pump was connected to a flexible infusion tube to deliver the NaOH solution into the precursor solution.

A DC dimmer was used to regulate the pump speed, enabling continuous adjustment of flow rate. The system was assembled to ensure vertical delivery of the precipitating agent into the reaction medium to minimize splashing and local turbulence. Prior to synthesis, the peristaltic pump was calibrated to establish a quantitative relationship between applied voltage and volumetric flow rate.

5.3. Peristaltic Pump Calibration and Flow-Rate Determination

Flow-rate calibration was performed by measuring the volume of liquid delivered over a fixed time interval at different applied voltages. The flow rate (Q) was calculated using Equation 1.

$$Q = \frac{V}{t} \tag{1}$$

where V is the collected volume (µL) and t is time (s). For each voltage setting, measurements were repeated, and the average value with standard deviation was calculated. The stability of the flow rate was evaluated through: Flow rate vs. time; Flow rate vs. cumulative volume; Volume vs. time. Linear regression analysis was performed to determine the coefficient of determination (R^2), which reflects flow stability and reproducibility.

5.4. Synthesis of ZnO Nanoparticle

The synthesis process began with the preparation of the Zinc Acetate Dihydrate and NaOH solutions by stoiciometry reaction (Eq. 2). These solutions were then mixed together using the hotplate and magnetic stirrer with room temperature and 2000 rpm. The peristaltic pump, connected to the infusion tube, was used to control the flow rate of the NaOH solution into Zinc Acetate Dihydrate solution. The voltage controller and power supply were used to regulate the operation of the peristaltic pump. The entire process was carefully monitored to ensure consistency and precision. White percipitate was rinsed by distilled water until pH 7. Then, the percipitate was dry in the oven at 100°C.

$$Zn(CH_3COO)_2.2H_2O + 2NaOH \rightarrow ZnO + 2NaCH_3COO + H_2O \qquad (2)$$

5.5. Characterization

The structural properties of the synthesized ZnO nanoparticles were characterized using X-ray diffraction (XRD) to determine phase composition, crystallinity, and crystallite size. The crystallite size was estimated using the Scherrer equation based on the full width at half maximum (FWHM) of the diffraction peaks. Morphological analysis was conducted using scanning electron microscopy (SEM) to observe particle shape, size distribution, and surface features.

6. Results and Discussion

The implementation of a peristaltic pump in the co-precipitation system enabled controlled and continuous delivery of the precipitating agent, addressing a key limitation of conventional dropwise methods [15], [16]. The modified system utilized an infusion tube integrated with a peristaltic pump operating under a regulated DC voltage (Figure 1). Calibration results demonstrated that at an applied voltage of 2.28 V, the system produced an average flow rate of 93.39 ± 1.39 µL/s, indicating high precision. The relationship between flow rate and time, as well as cumulative volume, exhibited excellent linearity with a coefficient of determination (R^2 = 0.99946), confirming the stability and reproducibility of the system. Such near-ideal linear behavior indicates that the peristaltic pump is capable of delivering a constant volumetric flow, which is essential for maintaining uniform reaction conditions during nanoparticle synthesis.

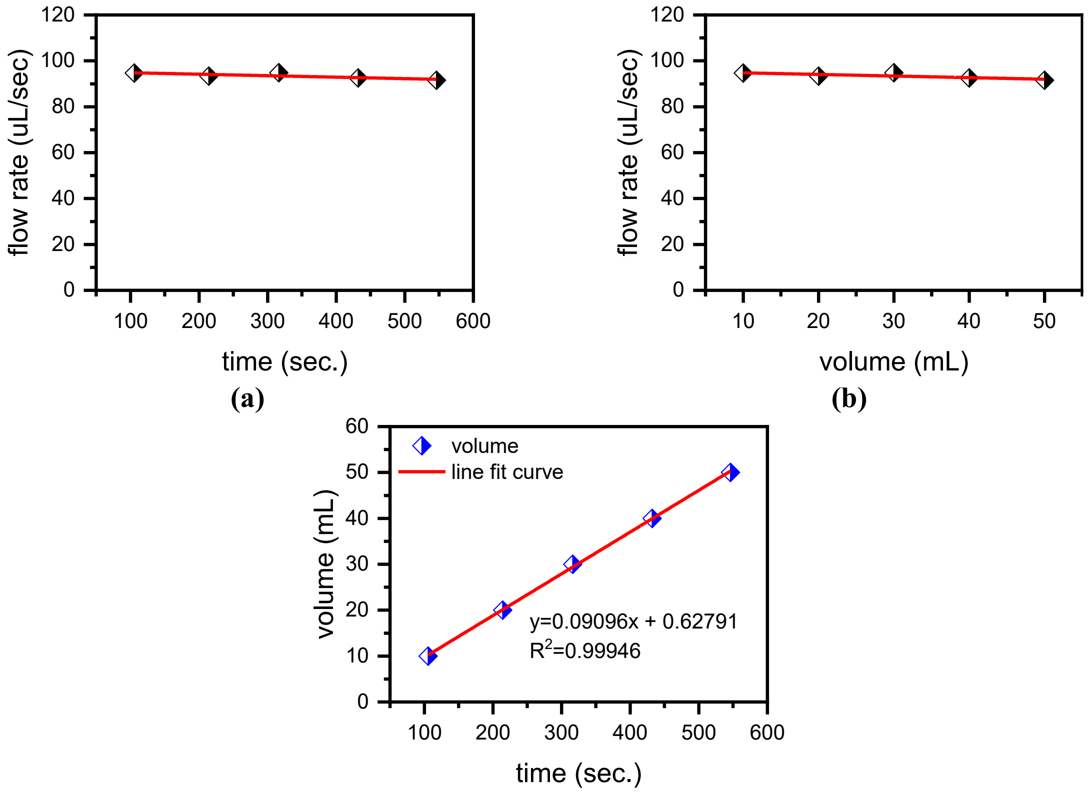

Figure 1. Flow stability testing of the peristaltic pump: (a) flow rate vs. time, (b) flow rate vs. volume, and (c) volume vs. time.

The stability of the flow rate plays a critical role in controlling supersaturation dynamics during the co-precipitation process [16]. In conventional systems, fluctuations in reactant addition often lead to localized supersaturation spikes, resulting in uncontrolled nucleation and particle agglomeration. In contrast, the controlled flow provided by the peristaltic pump ensures a gradual and uniform increase in hydroxide ion concentration, thereby promoting homogeneous nucleation. This controlled environment reduces secondary nucleation events and enables more uniform particle growth, ultimately improving reproducibility across synthesis batches.

The structural properties of the synthesized ZnO nanoparticles were analyzed using X-ray diffraction (XRD) (Figure 2a). The diffraction patterns confirmed the formation of a single-phase ZnO structure with no detectable secondary phases or impurities. All observed peaks correspond well with the standard hexagonal wurtzite structure (space group *P 6 3 m c*), consistent with the Crystallography Open Database (COD No. 9004178) [17]. The lattice parameters were determined to be a=b=3.2493 Å and c=5.2057 Å, which are in good agreement with reported values for bulk ZnO. The high degree of matching, reflected by a figure of merit (*FoM*) of 0.99, indicates excellent crystallinity and phase purity of the synthesized material.

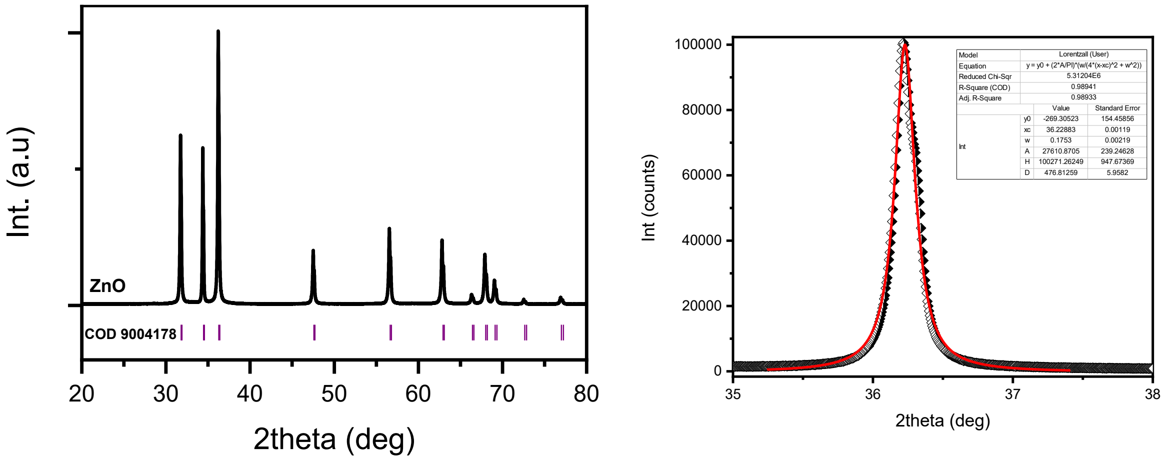

Model	Lorentzall (User)		
Equation	y = y0 + (2*A/PI)*(w/(4*(x-xc)^2 + w^2))		
Reduced Chi-Sqr	5.31204E6		
R-Square (COD)	0.98941		
Adj. R-Square	0.98933		
		Value	Standard Error
Int	y0	-269.30523	154.45856
	xc	36.22883	0.00119
	w	0.1753	0.00219
	A	27610.8705	239.24628
	H	100271.26249	947.67369
	D	476.81259	5.9582

(a) **(b)**

Figure 2. (a) XRD pattern of ZnO and matching COD 9004178 and (b) Lorentzian fit for peak fitting

Based on the XRD data, the crystal size of ZnO nanoparticles obtained using the Scherrer equation as in the Equation 3.

$$D_{hkl} = \frac{k\lambda}{\beta \cdot \cos\theta} \tag{3}$$

where D_{hkl} is the crystal size in the hkl plane, k is the structure factor (0.9), β is the Full Width at Half Maximum (FWHM), and θ is the position of the Bragg angle. FWHM is obtained by curve fitting using the Lorentz equation as shown in Figure 2b. Table 1 shows the results of calculating the crystal size of ZnO nanoparticles in various methods.

Table 1. Crystallite size of ZnO Nanoparticles

No.	**hkl**	**Crystallite size (nm)**
1	1 0 0	61.74
2	0 0 2	76.16
3	1 0 1	59.89
4	1 0 2	55.23
5	2 -1 0	52.10
6	2 0 0	51.62
7	1 0 3	47.05
8	2 -1 2	48.98
9	2 0 1	49.15
10	0 0 4	60.83
11	2 0 2	53.03
Average ± SD		**55.98 ± 8.35**

Crystallite size analysis based on XRD peak broadening revealed an average size of 55.98 ± 8.35 nm across multiple diffraction planes. The relatively narrow standard deviation suggests a uniform crystallite size distribution, which can be attributed to the stable nucleation conditions achieved through controlled flow rate [16]. Compared to typical co-precipitation methods reported in the literature, where broader size distributions are often observed due to inconsistent mixing, the present method demonstrates improved control over crystal growth. This result supports the hypothesis that flow-rate regulation directly influences nucleation kinetics and growth uniformity.

Morphological characterization using scanning electron microscopy (SEM) revealed the formation of ZnO nanorods with elongated structures and relatively high aspect ratios. The formation of such anisotropic structures is commonly associated with preferential growth along the c-axis of the hexagonal ZnO crystal. In this study, the controlled addition of the precipitating agent likely facilitated a steady supply of hydroxide ions, promoting directional crystal growth while suppressing random aggregation. This observation is consistent with previous reports indicating that controlled reaction environments favor the formation of well-defined nanostructures.

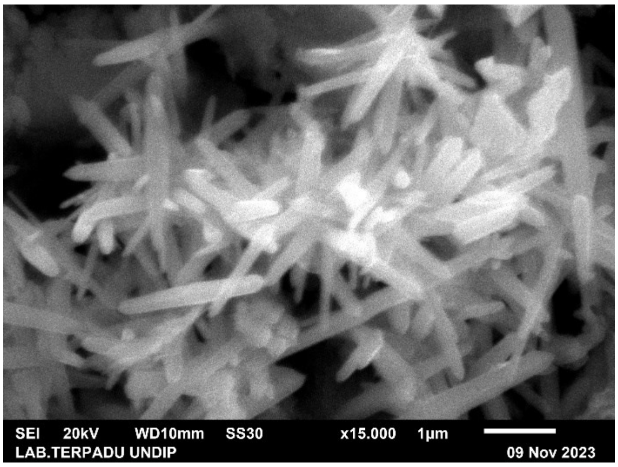

Figure 4. SEM image of ZnO nanorods

When compared with previous studies, variations in ZnO morphology such as nanosheets, aggregated particles, or irregular nanorods have been attributed to differences in synthesis parameters, particularly mixing conditions and reactant addition rates. Studies by Aljaafari (2020) and Thein et al. (2015) reported that uncontrolled co-precipitation often leads to heterogeneous morphologies due to rapid supersaturation and uneven nucleation [18], [19]. In contrast, the present study demonstrates that flow-rate stabilization serves as a governing parameter in achieving uniform nanorod structures. This highlights the importance of hydrodynamic control in wet-chemical synthesis routes. These variations in morphology can significantly influence the photocatalytic performance of ZnO, highlighting the importance of controlling the synthesis conditions to achieve the desired nanoparticle morphology [20], [21].

Overall, the results clearly indicate that integrating a peristaltic pump into the co-precipitation process significantly enhances control over reaction kinetics, structural properties, and morphology of ZnO nanoparticles. The high stability of the flow rate contributes directly to improved reproducibility and product quality. These findings establish flow-rate regulation as a critical parameter in nanoparticle synthesis and provide a scalable strategy for producing high-quality ZnO nanostructures with controlled properties.

7. Conclusion

This study successfully demonstrates that the integration of a peristaltic pump into the co-precipitation process provides a reliable and effective approach for controlling the synthesis of ZnO nanoparticles. The calibrated system exhibited highly stable flow characteristics, as evidenced by a near-linear relationship between flow rate and time ($R^2 = 0.99946$), ensuring consistent reaction conditions. Structural analysis confirmed the formation of single-phase hexagonal ZnO with high crystallinity, while crystallite size analysis indicated a relatively uniform distribution (55.98 ± 8.35 nm).

Morphological observations revealed the formation of nanorod structures, which are attributed to controlled supersaturation and directional crystal growth facilitated by stable reactant addition. These results highlight the critical role of flow-rate regulation in governing nucleation kinetics and particle growth in co-precipitation systems. The proposed method offers a low-cost, scalable, and reproducible strategy for nanoparticle synthesis. Future work should focus on systematic variation of flow rate, incorporation of functional property evaluation, and extension of this approach to other metal oxide systems to further validate its applicability and enhance its impact.

Acknowledgment

We would like to express our deepest gratitude to Universitas Palangka Raya and LPPM (Lembaga Penelitian dan Pengabdian kepada Masyarakat) for their financial support of this research through the PNBP funds, contract number 0699/UN24.13/AL.04/2023.

References

[1] Nasikhudin, M. Diantoro, A. Kusumaatmaja, dan K. Triyana, "Enhancing photocatalytic performance by sonication and surfactant addition on the synthesis process of PVA/TiO2nanofibers membranes by electrospinning method," *AIP Conf. Proc.*, vol. 2251, no. August, 2020, doi: 10.1063/5.0017654.

[2] M. Diantoro *et al.*, "Potential of nanooxidic materials and structures of photoanodes for DSSCs," *Energy Mater. Fundam. to Appl.*, hal. 213–247, 2021, doi: 10.1016/B978-0-12-823710-6.00013-3.

[3] L. Zhang *et al.*, "Ultrasound-Assisted Synthesis of Potentially Food-Grade Nano-Zinc Oxide in Ionic Liquids: A Safe, Green, Efficient Approach and Its Acoustics Mechanism," *Foods*, vol. 11, no. 11, hal. 1656, Jun 2022, doi: 10.3390/foods11111656.

[4] M. Diantoro, M. B. Zaini, T. Suprayogi, N. Mufti, S. Zulaikah, dan A. Hidayat, "Effect of (SnO<inf>2</inf>:TiO<inf>2</inf>) nanoparticles on charging performance of integrated dye-sensitized solar cell-supercapacitor," in *AIP Conference Proceedings*, 2020, vol. 2231, doi: 10.1063/5.0002438.

[5] I. Luthfiyah *et al.*, "The effect of spincoating speed on ZnONR microstructure and it's potential of ZnONR/Aluminum foil electrodes symmetric supercapacitors," *J. Phys. Conf. Ser.*, vol. 1595, no. 1, hal. 012001, 2020, doi: 10.1088/1742-6596/1595/1/012001.

[6] N. Mufti *et al.*, "Photoelectrochemical Performance of ZnO Nanorods Grown on Stainless Steel Substrate," in *IOP Conference Series: Materials Science and Engineering*, 2019, vol. 515, no. 1, doi: 10.1088/1757-899X/515/1/012023.

[7] I. Iwantono, S. K. Md Saad, F. Anggelina, A. Awitdrus, M. A. Ramli, dan A. A. Umar, "Enhanced charge transfer activity in Au nanoparticles decorated ZnO nanorods photoanode," *Phys. E Low-dimensional Syst. Nanostructures*, vol. 111, hal. 44–50, Jul 2019, doi: 10.1016/j.physe.2019.03.001.

[8] A. Gnanaprakasam, V. M. Sivakumar, P. L. Sivayogavalli, dan M. Thirumarimurugan, "Characterization of TiO<inf>2</inf> and ZnO nanoparticles and their applications in photocatalytic degradation of azodyes," *Ecotoxicol. Environ. Saf.*, vol. 121, hal. 121–125, 2015, doi: 10.1016/j.ecoenv.2015.04.043.

[9] A. Hidayat *et al.*, "Synthesis and characterization of TiO2/ZnO-Ag@TiO2nanocomposite and their performance as photoanode of organic Dye-Sensitized Solar Cell," *Mater. Today Proc.*, vol. 44, no. xxxx, hal. 3395–3399, 2020, doi: 10.1016/j.matpr.2020.11.862.

[10] N. A. Salahuddin, M. El-Kemary, dan E. M. Ibrahim, "Synthesis and characterization of ZnO nanoparticles via precipitation method: effect of annealing temperature on particle size," *Nanosci. Nanotechnol.*, vol. 5, no. 4, hal. 82–88, 2015.

[11] B. Andersson, R. Andersson, L. Håkansson, M. Mortensen, R. Sudiyo, dan B. van Wachem, *Turbulent mixing and chemical reactions*. 2012.

[12] S. M. D'Addio dan R. K. Prud'homme, "Controlling drug nanoparticle formation by rapid precipitation," *Adv. Drug Deliv. Rev.*, vol. 63, no. 6, hal. 417–426, 2011, doi: 10.1016/j.addr.2011.04.005.

[13] A. Rezaei, E. Katoueizadeh, dan S. M. Zebarjad, "Investigation of the parameters affecting the morphology of zinc oxide (ZnO) nanoparticles synthesized by precipitation method," *Mater.*

Today Chem., vol. 26, 2022, doi: 10.1016/j.mtchem.2022.101239.

[14] M. O. B. A *et al.*, “Co-precipitation synthesis of stable iron oxide nanoparticles with NaOH: New insights and continuous production via flow chemistry,” *Chem. Eng. J.*, vol. 399, 2020.

[15] A. K. Patel *et al.*, “Design and Fabrication of Infusion Pump to Control the Flow Rate of Solution for Synthesis of Zinc Oxide Nanomaterial,” *Int. J. Appl. Eng. Res.*, vol. 14, no. 5, hal. 1091–1097, 2019.

[16] M. L. Popa, M. D. Preda, I. A. Neacșu, A. M. Grumezescu, dan O. Ginghină, “Traditional vs. Microfluidic Synthesis of ZnO Nanoparticles,” *Int. J. Mol. Sci.*, vol. 24, no. 3, 2023, doi: 10.3390/ijms24031875.

[17] T. Suprayogi, M. Z. Masrul, M. Diantoro, A. Taufiq, A. Fuad, dan A. Hidayat, “The Effect of Annealing Temperature of ZnO Compact Layer and TiO 2 Mesoporous on Photo-Supercapacitor Performance,” *IOP Conf. Ser. Mater. Sci. Eng.*, vol. 515, hal. 012006, Apr 2019, doi: 10.1088/1757-899X/515/1/012006.

[18] A. Aljaafari, “Size Dependent Photocatalytic Activity of ZnO Nanosheets for Degradation of Methyl Red,” *Front. Mater.*, vol. 7, Nov 2020, doi: 10.3389/fmats.2020.562693.

[19] M. T. Thein, S.-Y. Pung, A. Aziz, dan M. Itoh, “Stacked ZnO nanorods synthesized by solution precipitation method and their photocatalytic activity study,” *J. Sol-Gel Sci. Technol.*, vol. 74, no. 1, hal. 260–271, Apr 2015, doi: 10.1007/s10971-015-3646-z.

[20] P. K. Aspoukeh, A. A. Barzinjy, dan S. M. Hamad, “Synthesis, properties and uses of ZnO nanorods: a mini review,” *Int. Nano Lett.*, vol. 12, no. 2, hal. 153–168, Jun 2022, doi: 10.1007/s40089-021-00349-7.

[21] S. Raha dan M. Ahmaruzzaman, “ZnO nanostructured materials and their potential applications: progress, challenges and perspectives,” *Nanoscale Adv.*, vol. 4, no. 8, hal. 1868–1925, 2022, doi: 10.1039/D1NA00880C.